Am J Physiol Cell Physiol
279: C1123–C1134, 2000.

Upregulation of Kv1.3 K^+ channels in microglia deactivated by TGF-β

TOM SCHILLING,[1] FRED N. QUANDT,[2] VLADIMIR V. CHERNY,[2] WEI ZHOU,[2]
UWE HEINEMANN,[1] THOMAS E. DECOURSEY,[2] AND CLAUDIA EDER[1]
[1]*Institut für Physiologie der Charité, Humboldt Universität, D 10117 Berlin, Germany; and*
[2]*Department of Molecular Biophysics and Physiology, Rush Presbyterian St. Luke's Medical Center, Chicago, Illinois 60612*

Received 2 February 2000; accepted in final form 26 April 2000

Schilling, Tom, Fred N. Quandt, Vladimir V. Cherny, Wei Zhou, Uwe Heinemann, Thomas E. DeCoursey, and Claudia Eder. Upregulation of Kv1.3 K^+ channels in microglia deactivated by TGF-β. *Am J Physiol Cell Physiol* 279: C1123–C1134, 2000.—Microglial activation is accompanied by changes in K^+ channel expression. Here we demonstrate that a deactivating cytokine changes the electrophysiological properties of microglial cells. Upregulation of delayed rectifier (DR) K^+ channels was observed in microglia after exposure to transforming growth factor-β (TGF-β) for 24 h. In contrast, inward rectifier K^+ channel expression was unchanged by TGF-β. DR current density was more than sixfold larger in TGF-β-treated microglia than in untreated microglia. DR currents of TGF-β-treated cells exhibited the following properties: activation at potentials more positive than −40 mV, half-maximal activation at −27 mV, half-maximal inactivation at −38 mV, time dependent and strongly use-dependent inactivation, and a single channel conductance of 13 pS in Ringer solution. DR channels were highly sensitive to charybdotoxin (CTX) and kaliotoxin (KTX), whereas α-dendrotoxin had little effect. With RT-PCR, mRNA for Kv1.3 and Kir2.1 was detected in microglia. In accordance with the observed changes in DR current density, the mRNA level for Kv1.3 (assessed by competitive RT-PCR) increased fivefold after treatment of microglia with TGF-β.

brain macrophages; transforming growth factor-β; inward rectifier K^+ current; delayed rectifier K^+ current; reverse transcription-polymerase chain reaction; Kir2.1

MICROGLIA REPRESENT A POPULATION of resident macrophages of the brain. In addition to performing normal functions of macrophages in other tissues, microglia are highly specialized. Resting microglia are highly ramified, with extensive processes that presumably act as antennae, sensing inflammatory stimuli, tissue damage, cellular debris, etc. They are characterized by downregulated macrophage surface antigens and macrophage functions. On stimulation, microglia react by withdrawing their processes, becoming ameboid and macrophage-like. Activated microglia become capable of phagocytosis, proliferation, and chemotaxis and release various cytokines and cytotoxins (34, 39, 40). Recent interest in microglia has been piqued by the idea that hyperactive microglia may cause tissue damage, possibly contributing to lesions of human immunodeficiency virus-associated dementia (32), multiple sclerosis (42), Alzheimer's disease (28), and a variety of other neurodegenerative and autoimmune diseases (34, 39, 40). This background emphasizes the importance of understanding microglial deactivation, the reversal of microglial activation.

Electrophysiological studies in vitro have revealed dramatic changes in the expression levels of K^+ channels in microglia during the process of activation (for review, see Ref. 10). Exposure to a variety of activating stimuli produces a similar pattern of electrophysiological changes in microglia. Lipopolysaccharide (LPS) (31), granulocyte-macrophage colony-stimulating factor (GM-CSF) (11, 13), or interferon-γ (IFN-γ) (13) induces upregulation of delayed rectifier (DR) K^+ currents, which is accompanied by simultaneous downregulation of inward rectifier (IR) K^+ currents. The DR K^+ currents of cytokine- or LPS-activated microglial cells share many properties with cloned Kv1.3 channels, including an activation threshold at about −40 mV, strongly use-dependent inactivation, and a high sensitivity to the scorpion peptide toxins CTX, KTX, and noxiustoxin (11, 31). On cellular activation, upregulation of DR (Kv1.3) K^+ currents also occurs in other immune cells, such as macrophages and lymphocytes (for review, see Ref. 7). Effects of deactivating cytokines on microglial K^+ channel expression have not yet been investigated.

Several studies have demonstrated that TGF-β plays an important role in deactivation of microglia. For example, TGF-β1 has been shown to suppress superoxide production in LPS-activated microglial cells and to reduce expression of Fc receptors and major histocompatibility complex class II molecules in IFN-γ-stimulated microglia (14, 23, 27, 29, 41). TGF-β is produced in the central nervous system. Microglial cells express TGF-β receptors and are capable of releasing TGF-β1

Address for reprint requests and other correspondence: C. Eder, Institut für Physiologie der Charité, Humboldt Universität, Tucholskystr. 2, D 10117 Berlin, Germany (E-mail: claudia.eder@charite.de).

The costs of publication of this article were defrayed in part by the payment of page charges. The article must therefore be hereby marked "*advertisement*" in accordance with 18 U.S.C. Section 1734 solely to indicate this fact.

 0363-6143/00 $5.00 Copyright © 2000 the American Physiological Society

(5). In microglia, TGF-β reduces production of various proinflammatory cytokines, such as interleukin (IL)-1, IL-6, and tumor necrosis factor-α, and inhibits proliferation (20, 41).

In the present study we investigated the patterns of K^+ channel expression in microglia before and after exposure to the deactivating cytokine TGF-β. The inward and outward rectifier K^+ currents of TGF-β-treated microglial cells were characterized, and the molecular identities of the main K^+ channels were determined. Preliminary accounts of this work have been published in abstract form (35, 36).

MATERIALS AND METHODS

Cell Culture

Primary and secondary microglial cultures. Microglia were obtained from brain cell cultures of newborn NMRI mice, supplied by Charles River (Sulzfeld, Germany). Mixed brain cell cultures were prepared as described previously (12). Brain cortices were enzymatically dissociated (15 min at 37°C with 0.25% trypsin, type XI, Sigma), and a single cell suspension was achieved by repeated triturations. Cells were seeded into tissue culture flasks at a density of $2–4 \times 10^6$/10 ml in DMEM (GIBCO) supplemented with 10% heat-inactivated FCS (GIBCO) and 30% supernatant of L-929 fibroblasts as a source of macrophage CSF (M-CSF). After at least 10 days of incubation, microglia were harvested by shaking the cultures (30 min, 300 rpm) to detach weakly adherent cells from the astrocytic monolayer. Isolated microglia were seeded on glass coverslips in 24-well Costar plates (3×10^4/0.5 ml). These cells were cultured in DMEM supplemented with 10% FCS. The culture medium did not contain M-CSF. In secondary culture, untreated microglial cells were partially activated, i.e., cells exhibited an ameboid morphology and the expression of various macrophage surface antigens was upregulated (12). One to two days after the isolation procedure, microglial cells were treated with 10 ng/ml recombinant human TGF-β1 or 10 ng/ml natural porcine TGF-β2 (both from Sigma) to induce deactivation. Patch-clamp recordings were performed 24 h after the TGF-β treatment.

BV-2 microglial cell line. The immortalized mouse microglial cell line BV-2, which exhibited properties similar to activated microglia (Refs. 1 and 2; kindly provided by Dr. E. Blasi, Perugia, Italy), was used in some experiments. BV-2 microglial cells were cultured permanently in DMEM supplemented with 10% FCS and 2 mM L-glutamine. BV-2 cells were split twice a week and were plated on glass coverslips at a density of $1–1.5 \times 10^4$/0.5 ml for subsequent patch-clamp experiments. To induce deactivation, BV-2 cells were treated for 24 h with 10 ng/ml TGF-β1 or TGF-β2.

Electrophysiological Recordings

Whole cell measurements. Whole cell membrane currents were measured using an EPC-9 patch-clamp amplifier (HEKA, Lambrecht/Pfalz). The amplifier was interfaced to an IBM computer for pulse application and data recording. Series resistance compensation was routinely used to reduce the effective series resistance by ~70%. Patch electrodes of 2–4 MΩ were fabricated on a two-stage puller (Narishige PP-83, Tokyo, Japan) from borosilicate glass (outer diameter 1.5 mm and inner diameter 1 mm; Hilgenberg, Malsfeld, Germany). The electrodes were filled with the following solution (in mM): 120 KCl, 1 $CaCl_2$, 2 $MgCl_2$, 10 HEPES, and 11 EGTA. This solution was adjusted to pH 7.3 with KOH. The extracellular solution contained (in mM) 130 NaCl, 5 KCl, 2 $CaCl_2$, 1 $MgCl_2$, 10 HEPES, and 8 D-glucose. The pH of the extracellular solutions was adjusted to 7.4 with NaOH. All recordings were done at room temperature (20–23°C). Whole cell K^+ currents were filtered at 3 kHz and stored on computer disk for subsequent analyses. Analyses were performed on IBM computers with the Pulse/PulseFit program (HEKA, Lambrecht/Pfalz). Data are presented as mean values ± SE. The number of experiments is indicated. Membrane capacitances of the cells analyzed in this study varied between 5 and 44 pF. In morphologically complex cells such as microglia, long, narrow processes may not be under voltage-clamp control. The cells studied here typically had one or two short processes, probably comprising a small fraction of the total membrane area. Although we did not observe electrophysiological manifestations of significant space-clamp problems, we cannot rule out the possibility that some small and inaccessible regions of membrane were excluded electrically from contributing to the whole cell currents. If not stated otherwise, leak currents were subtracted from current records before further analysis. Leak current was determined by measuring the current evoked by a voltage step from −60 to −70 mV where no time-dependent current was present. Leak current was subtracted from each K^+ current recording assuming a linear current-voltage relationship of the leak currents.

Single channel recordings. Single channel experiments were done at 20°C, with the bath temperature controlled by Peltier devices. Micropipettes were pulled in several stages using a Flaming Brown automatic pipette puller (Sutter Instruments, San Rafael, CA) from 7052 or KG-12 glass (Garner Glass, Claremont, CA), coated with Sylgard 184 (Dow Corning, Midland, MI), and heat polished to a tip resistance usually 3–15 MΩ. Electrical contact with the pipette solution was achieved by a thin sintered Ag-AgCl pellet (In Vivo Metric Systems, Healdsburg, CA) attached to a silver wire covered by a Teflon tube or simply with a chlorided silver wire. A reference electrode made from a Ag-AgCl pellet was connected to the bath through an agar bridge made with Ringer solution. The current signal from the patch clamp (List Electronic, Darmstadt, Germany, Axopatch-1A or Axopatch 200B; Axon Instruments, Foster City, CA) was digitized and stored in computer files for offline analysis using Indec Laboratory Data Acquisition and Display Systems (Indec, Sunnyvale, CA) or pCLAMP 6.0.3 (Axon Instruments). Data acquisition and analysis programs were written in BASIC-23 or FORTRAN. Data are presented without correction for liquid junction potentials.

Pipettes were filled with several different solutions: Ringer solution (in mM: 160 NaCl, 4.5 KCl, 2 $CaCl_2$, 1 $MgCl_2$, 5 HEPES, titrated to pH 7.4 with NaOH), KF + KCl (in mM: 70 KCl, 40 KF, 1 $CaCl_2$, 11 EGTA, 20 HEPES, titrated to pH 7.35 using KOH), and KCl internal (in mM: 120 KCl, 1 $CaCl_2$, 2 $MgCl_2$, 10 HEPES, 11 EGTA, titrated to pH 7.35 with KOH). The bath solutions included Ringer solution, K-Ringer solution (in mM: 160 KCl, 2 $CaCl_2$, 1 $MgCl_2$, 10 HEPES, titrated to pH 7.4 with KOH), $KMeSO_3^-$ (68 $KMeSO_3^-$, 100 *N*,*N*-bis[2-hydroxyethyl]-2-aminoethanesulfonic acid, 2 $MgCl_2$, 1 EGTA, titrated to pH 7.0 with KOH), and some of the pipette solutions.

Cell-attached and excised, inside-out or outside-out patches (17) were studied. The seal was formed with Ringer solution in the bath, which was replaced with isotonic K^+-Ringer or $KMeSO_3^-$ solution for cell-attached patch recording. We assume that the membrane potential was "clamped" near 0 mV by this procedure. Inside-out patches were formed

by lifting the pipette into the air briefly. Outside-out patches were formed by lifting the pipette from the cell after achieving whole cell configuration.

Currents and voltages are presented in the normal sense; that is, upward currents represent current flowing outward through the patch membrane from the original intracellular surface, and potentials are expressed by defining as 0 mV the solution facing the original extracellular membrane surface. Cell-attached patch data are expressed on the assumption that the membrane potential of the cell was 0 mV when isotonic K^+ solutions were present in the bath.

Data analyses. The steady-state activation curve was fitted using the following Boltzmann equation

$$g/g_{max} = \{1 + \exp[(V_{1/2} - V_{test})/k]\}^{-1}$$

in which g is the peak chord conductance value at each potential, g_{max} is the maximal conductance, $V_{1/2}$ is the voltage at which the current is half activated, V_{test} is the test potential, and k is a factor describing the steepness of the activation curve.

The inactivation data were fitted using the following Boltzmann equation

$$I/I_{max} = \{1 + \exp[(V_{hold} - V_{1/2})/k]\}^{-1}$$

in which I_{max} is the maximum current, $V_{1/2}$ is the voltage at which the current is half inactivated, and V_{hold} is the voltage of the conditioning holding potential.

Time constants of activation and inactivation of DR currents were determined using a Hodgkin-Huxley-type n^4j model (18) of the following form

$$I = I_{max}(1 - e^{-t/\tau_n})^4 e^{-t/\tau_j} + I_l$$

where I is the total current, I_l is the time-independent leak current, τ_n is the time constant of activation, and τ_j is the time constant of inactivation.

Pharmacological Studies

For drug application, a four-barrel microperfusion pipette was positioned at a distance of ~30–50 μm from the recorded cell to permit a rapid exchange of solutions outside the cell, which was achieved in <1 s. The flow rate was adjusted by hydrostatic pressure.

Effects of the following drugs were studied: CTX, α-dendrotoxin (α-DTX), and KTX (all from Latoxan, Rosans, France) and $BaCl_2$ and δ-DTX (both from Sigma). Peptide toxins were dissolved in 0.1% bovine serum albumin-containing solutions.

Statistics

The statistical significance of differences between experimental groups was evaluated by Student's *t*-test using the SPSS program. Data were considered to be statistically significant with $P < 0.05$.

RT-PCR

RNA isolation. Total RNA was isolated from cultured BV-2 cells using a modification of the procedure given by Chomczynski (4). Approximately 2×10^6 cells were centrifuged and resuspended in a minimum volume of growth medium. One milliliter of Trizol (GIBCO-Life Technologies) reagent was added. The manufacturer of Trizol specified subsequent steps in the isolation procedure that were followed. RNA was suspended in diethylpyrocarbonate-treated water and quantified by ultraviolet (UV) spectroscopy.

Reaction conditions. Tth polymerase was used to convert RNA to cDNA as well as to amplify cDNA by the PCR in the same reaction tube. Each reaction tube contained 100 ng total RNA and 5 units of polymerase. The RT step was carried out at 60°C for 30 min in the presence of Mn and the downstream gene-specific primer. Before PCR, a buffer that chelated Mn and substituted Mg was added along with the upstream gene-specific primer at 90°C. Thirty cycles of PCR were then performed using a combined annealing and extension step at a temperature of 60°C. Reaction products were visualized by gel electrophoresis. The gel contained 3% agarose, was stained with 10 μg/ml ethidium bromide, and subsequently destained. Oligonucleotide primers used in this study included those for mouse Kv1.3 (GenBank M30441, upstream 5′-ATCTTCAAGCTCTCCCGCCA, downstream 5′-CGATCACCATATACTCCGAC), glyceraldehyde-3-phosphate-dehydrogenase (G3PDH, Genebank M32599, upstream 5′-TGATGACATCAAGAAGGTGGTGAAG, downstream 5′-TCCTTGGAGGCCATGTAGGCCAT), mouse Kv1.5 (GenBank L22218, upstream 5′-GCCATTGCCATCGTGTCGGT, downstream 5′-ACATGTGGTCTCCACGATGA), and mouse Kir2.1 (GenBank X73052, upstream 5′-CGACTGCCATGACAACTCAA, downstream 5′-CATATCTCCGATTCTCGCCT).

Competitive RT-PCR. The abundance of specific species of mRNA (target) was determined using a competitive RT-PCR assay. In this assay, parallel RT-PCR reactions are performed. Each reaction tube contained a constant amount of total RNA and a variable amount of artificial RNA (competitor). The ratio of target to competitor was measured after RT-PCR to infer the amount of target in the reaction (37). The competitor was a truncated form of the target but contained the same primer binding sites. The concentration of this RNA competitor was measured by UV spectrophotometry.

The ratio of amplified target and competitor was determined from measurements of the intensity of the corresponding bands seen in the electrophoresis gel after staining. The intensity was measured from images digitized using a low-light integrating charge-coupled device camera. The relative intensity of each band was calculated as the sum of the values of all pixels in the band after subtraction of the background. The ability of each competitor to measure a change in mRNA abundance was tested by applying the assay to known dilutions of total RNA.

Restriction analysis. Products of RT-PCR were reamplified for restriction analysis and concentrated with a centrifugal filtration device. Digestion of the DNA was carried out in the appropriate buffer at 37°C for 1 h. *Hph* I was obtained from New England Biolabs. *Rsa* I and *Sac* I were obtained from Promega.

RESULTS

IR K^+ Currents in TGF-β-Treated Microglia

The effects of TGF-β on ionic currents were studied using the whole cell mode of the patch-clamp technique. Immediately after rupture of the cell membrane, the holding potential was set to −60 mV. To activate inward K^+ currents, cells were hyperpolarized to potentials between −70 and −150 mV for 200 ms. Voltage steps were applied in 10-mV increments. Figure 1 illustrates IR K^+ currents obtained from an untreated microglial cell (Fig. 1*A*) and from microglial cells that had been treated for 24 h with 10 ng/ml TGF-β1 (Fig. 1*B*) or 10 ng/ml TGF-β2 (Fig. 1*C*). There was no significant difference between the IR current density in untreated and TGF-β-treated microglia. At a potential of −150 mV, a mean IR current density was 10.7 ± 2.0

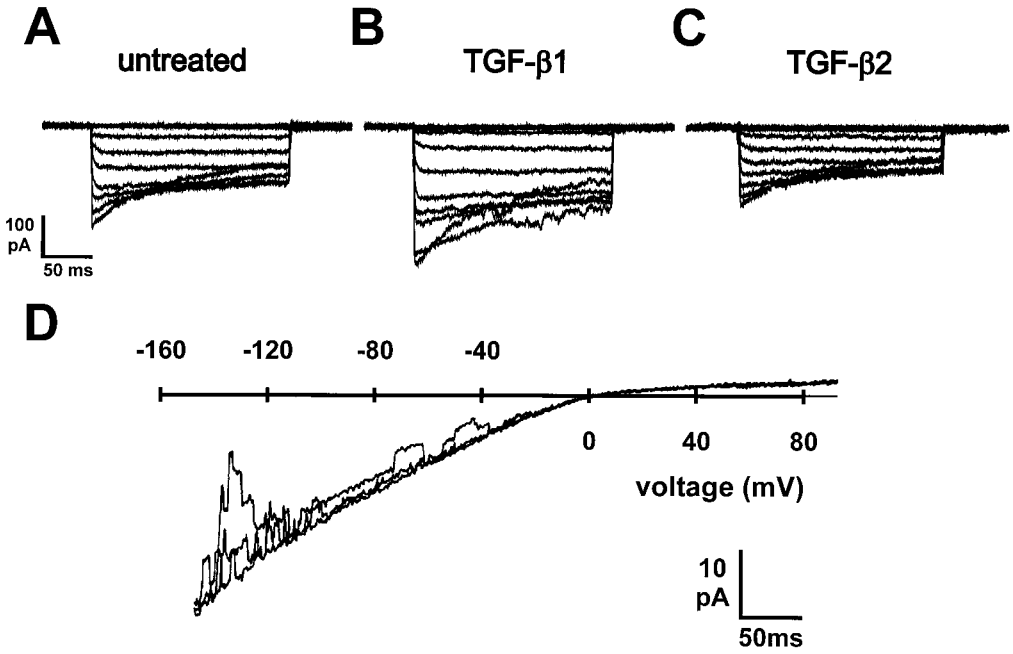

Fig. 1. Inward rectifier (IR) K^+ currents in untreated and transforming growth factor (TGF)-β-treated microglia. Pulses (200 ms) were applied from the holding potential (−60 mV) to potentials between −70 and −150 mV in 10-mV increments. *A*–*C*: leak-subtracted IR currents in an untreated microglial cell (*A*), in a microglial cell treated with 10 ng/ml TGF-β1 (*B*), and in a microglial cell exposed to 10 ng/ml TGF-β2 (*C*). *D*: IR K^+ channels in an excised, inside-out patch in approximately symmetrical K^+ solutions. Three consecutive ramp current records are superimposed, from voltage ramps applied from −160 to +80 mV. Pipette solution: KF+KCl; bath solution: KCl internal.

$\mu A/cm^2$ (mean ± SE, $n = 26$) in untreated microglia, similar to 10.9 ± 1.8 ($n = 31$) and 11.7 ± 3.5 $\mu A/cm^2$ ($n = 9$) in microglia treated with TGF-β1 or TGF-β2, respectively.

Single channel currents were recorded mainly from BV-2 cells. The changes in K^+ currents in BV-2 cells exposed to TGF-β for 1 day were similar to those observed in microglia in primary culture. When the pipette solution contained high extracellular K^+ concentration, most patches (13/18) contained IR channels, often at high density. Figure 1*D* illustrates ramp currents in an inside-out patch with at least five active IR channels. During voltage ramps, most of the IR channels were open at negative voltages, indicating a high open probability. No outward current other than leak was observed. Because of open-channel rectification, the value obtained for the conductance depended on the voltage range selected. Similar open-channel rectification has been observed in IR channels in endothelial cells (38). The single IR channel conductance obtained by linear regression on the averaged leak-subtracted open-channel current between −100 and −20 mV relative to the Nernst potential for K^+ was usually 25–30 pS.

In rat microglia, mRNA of both ROMK-1 and Kir2.1 channels was reported (25). To identify the IR channels that are expressed in TGF-β-treated murine microglia, we first investigated effects of extracellular Ba^{2+} on whole cell IR currents, because Kir2.1 channels are much more sensitive to Ba^{2+} than are ROMK-1 channels (24, 43). Micromolar concentrations of extracellular Ba^{2+} induced a voltage- and time-dependent blockade of IR currents (data not shown), and 1 mM Ba^{2+} abolished IR currents in TGF-β-treated microglia ($n = 10$) (Fig. 2, *A* and *B*). Next, we investigated effects of δ-DTX, a peptide toxin that inhibits ROMK-1 but no other IR channels (19). As shown in Fig. 2, *C* and *D*, neither the amplitude nor the kinetics of IR currents was affected by 100 nM δ-DTX ($n = 6$).

Whole Cell DR K^+ Currents in TGF-β-Treated Microglia

On membrane depolarization, voltage-gated outward K^+ currents were not detected in the majority of untreated microglia, as shown for the example in Fig. 3*A*. In contrast, all TGF-β-treated microglial cells exhibited a DR K^+ current when cells were depolarized to potentials more positive than −40 mV (Fig. 3, *B* and *C*). The mean density of DR currents in TGF-β1-treated microglia was more than six times larger than that in untreated microglial cells ($P < 0.001$). At +30 mV, the mean DR current densities were 31.8 ± 6.2 ($n = 56$) and 4.6 ± 0.8 $\mu A/cm^2$ ($n = 44$) in TGF-β1-treated microglia and in untreated microglia, respectively. A significant increase was also seen in microglia treated with TGF-β2, with a mean DR current density of 20.6 ± 4.4 $\mu A/cm^2$ ($n = 9$) ($P < 0.001$).

Single DR K^+ Channel Currents

Figure 4*A* shows a single averaged leak-subtracted current in a patch with one active DR channel. The slope conductance of the open-channel current at the reversal potential was 26 pS. In other patches, the single channel DR conductance was typically 25–30 pS in symmetrical high K^+ solutions. The properties used

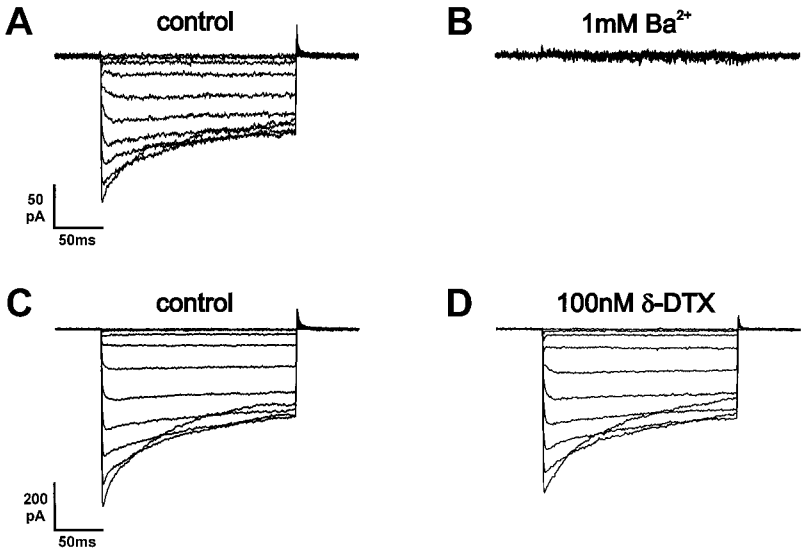

Fig. 2. Pharmacological properties of IR currents in TGF-β-treated microglia. Cells were hyperpolarized from −60 to −150 mV for 200 ms in 10-mV increments. *A* and *B*: IR currents were blocked completely during extracellular application of 1 mM Ba^{2+}. *C* and *D*: IR currents of TGF-β-treated microglia remained unchanged during superfusion with 100 nM δ-dendrotoxin (DTX). All currents are shown after leak subtraction.

to identify the single channels as DR included all of the following: activation with voltage in the general vicinity of −40 mV, inwardly rectifying open-channel current-voltage relationship in symmetrical K^+ solutions, flickery openings, and evidence of inactivation (during repeated trials the channels opened repeatedly followed by periods of inactivity).

Figure 4*B* illustrates the leak-subtracted current elicited by a voltage ramp in a cell-attached patch containing a single active DR channel. The bath contained K-Ringer solution, intended to "clamp" the resting membrane potential near 0 mV, and the pipette contained Ringer solution. The channel displays typical flickery openings, as well as inward rectification at large positive voltages (i.e., positive to +80 mV). The slope conductance estimated from the linear portion of the current-voltage relationship (below +60 mV) was variable both within one patch and between patches and ranged 8–17 pS. The average value from the seven most reliable patches studied with Ringer solution in the pipette was 12.6 ± 0.9 pS. Under similar conditions, the conductance of Kv1.3 channels in human lymphocytes is 13 pS (3).

Voltage Dependence of Activation and Inactivation of DR K^+ Currents

Kinetic and pharmacological properties of DR K^+ currents in TGF-β-treated cultured microglial cells were studied in the whole cell configuration. Figure 5*A* illustrates superimposed currents elicited by 200-ms pulses applied in 10-mV increments from the holding potential (−60 mV). DR currents were seen first at −30 mV and became larger at more depolarizing command voltages. After normalized peak conductances vs. membrane potential were plotted, the steady-state activation curve of DR currents could be described by a Boltzmann equation in TGF-β-treated microglia (Fig. 5*C*). Half-maximal activation occurred at −27 mV, with a slope factor, k, of 4.6 mV (n = 19).

The "steady-state" voltage dependence of inactivation of DR currents was studied by varying the holding potential between −90 and +20 mV in 10-mV increments. After the holding potential was established for at least 2 min, cells were pulsed to a test potential of +30 mV for 200 ms. When the holding potential was more positive than −60 mV, DR currents during the test pulse decreased in amplitude. As shown for the example of current recordings in Fig. 5*B*, DR current was not activated during the test pulse when cells were held at potentials positive to −20 mV. Peak amplitudes of the evoked currents were measured, normalized, and then plotted as a function of the holding potential (Fig. 5*C*). Fitted with a Boltzmann function, half-maximal inactivation was at −38 mV, with k = 4.3 mV (n = 13).

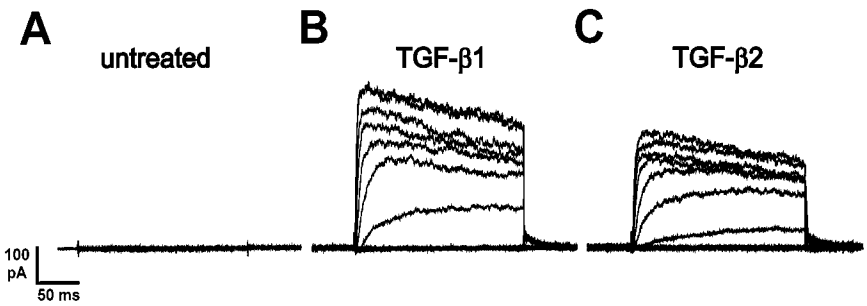

Fig. 3. Delayed rectifier (DR) K^+ currents in untreated and TGF-β-treated microglia. Microglial cells were depolarized from the holding potential of −60 mV to potentials between −50 and +30 mV for 200 ms in 10-mV increments. *A*–*C*: leak-subtracted currents in an untreated microglial cell (*A*), a microglial cell exposed to 10 ng/ml TGF-β1 (*B*), and a microglial cell exposed to 10 ng/ml TGF-β2 (*C*).

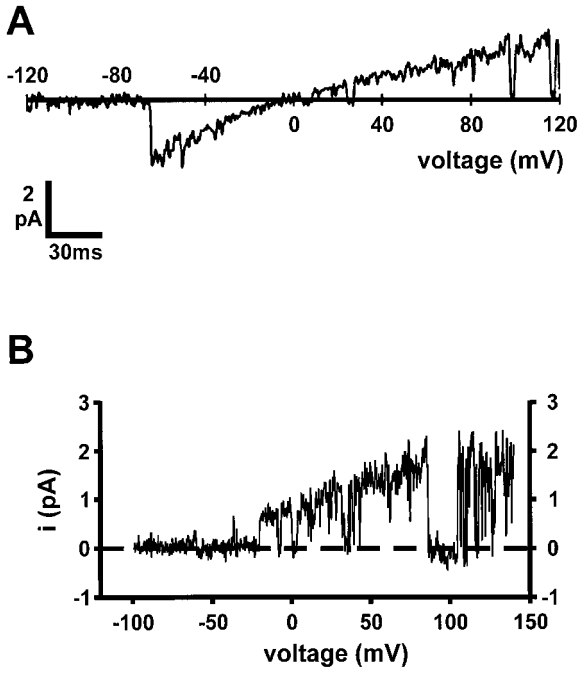

Fig. 4. Single DR channel currents. *A*: current recorded during a single voltage ramp in an inside-out patch from a BV-2 microglial cell. The average leak current obtained from other ramps when the channel was closed has been subtracted. Pipette contained KF + KCl, bath KCl internal solution. Ramp duration 0.3 s, filter 400 Hz. We held the cell at −100 mV for 1 s preceding each ramp. *B*: single DR channel current in a cell-attached patch from a BV-2 microglial cell with Ringer solution in the pipette. The average current from ramp records with no channel openings has been subtracted. The bath contained K-Ringer solution, which was assumed to clamp the resting membrane potential near 0 mV. Voltage of the conditioning holding potential (V_{hold}) = −80 mV, ramp rate 0.8 V/s, filter 1 kHz, sample rate 5 kHz.

Time-Dependent Activation and Inactivation of DR K^+ Currents

The activation time constant was determined by fitting n^4 kinetics (18) to the rising phase of DR current during voltage pulses to potentials between −40 and +30 mV. The activation time constant of DR currents was voltage dependent (Fig. 6, *A* and *B*), decreasing at more positive potentials. The activation time constant was 14.5 ± 2.2 ms at −30 mV, 2.4 ± 0.2 ms at 0 mV, and decreased less rapidly above 0 mV, reaching 1.3 ± 0.2 ms at +30 mV (n = 22).

To characterize the time dependence of inactivation of DR currents, 2,000-ms voltage pulses were applied to potentials between −40 and +30 mV. At potentials near the activation threshold, inactivation became faster with increasing depolarization. At potentials more positive than 0 mV, the inactivation rate did not change further (Fig. 6, *C* and *D*). The time constant of inactivation was 581 ± 40 ms (n = 13) at +30 mV.

Use Dependence of DR K^+ Currents

Pronounced use dependence of DR currents in TGF-β-treated microglial cells was apparent during 200-ms voltage commands to +30 mV applied at a frequency of 1 Hz (Fig. 7*A*). The amplitude of the DR current decreased rapidly during the first few pulses and thereafter continued to decline during subsequent pulses, without reaching a clear steady-state after 30 s. After 1-Hz stimulation for 30 s, the amplitude of DR currents was reduced by 71 ± 3% (n = 17) compared with the current during the first pulse. The time course of decay during 1-Hz repetitive stimulation was best fitted by two exponentials with time constants of 1.6 and 20.5 s (n = 17) (Fig. 7*B*).

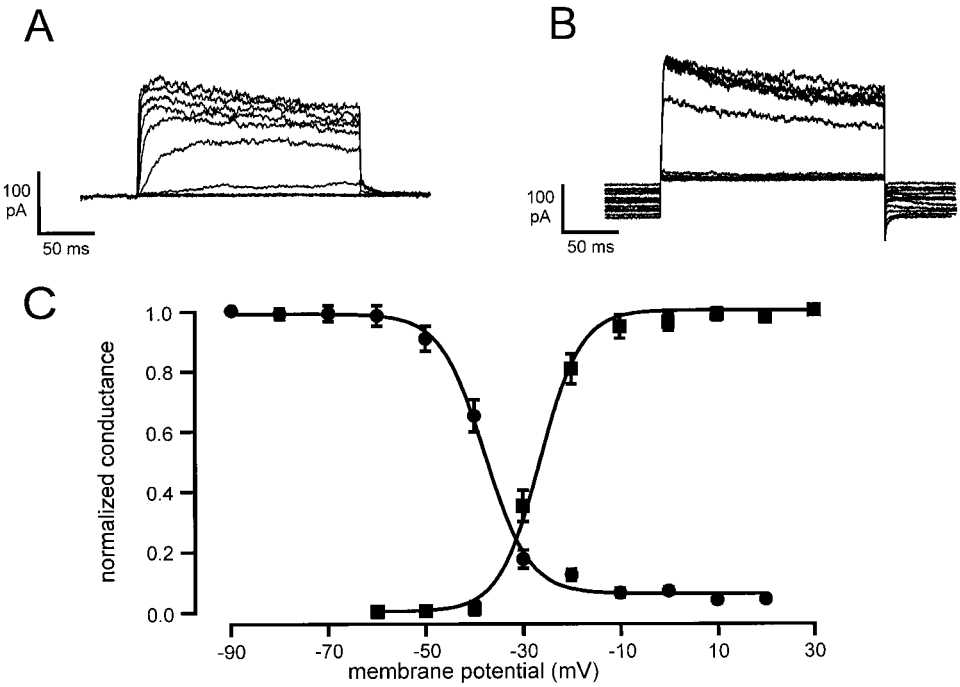

Fig. 5. Steady-state activation and inactivation of DR currents. *A*: to study activation, outward K^+ currents were evoked by 200-ms depolarizing voltage commands applied every 30 s in 10-mV steps from −60 to +30 mV. Cells were held at −60 mV. *B*: to quantitate inactivation, the holding potential was varied between −90 and +20 mV, and a 200-ms test pulse to +30 mV was applied. *C*: steady-state inactivation is indicated by the normalized peak test current (means ± SE; n = 13 for each data point) as illustrated in *B* (●) and steady-state activation is plotted as the normalized peak conductance (means ± SE; n = 19 for each data point) during pulses such as those in *A* (■).

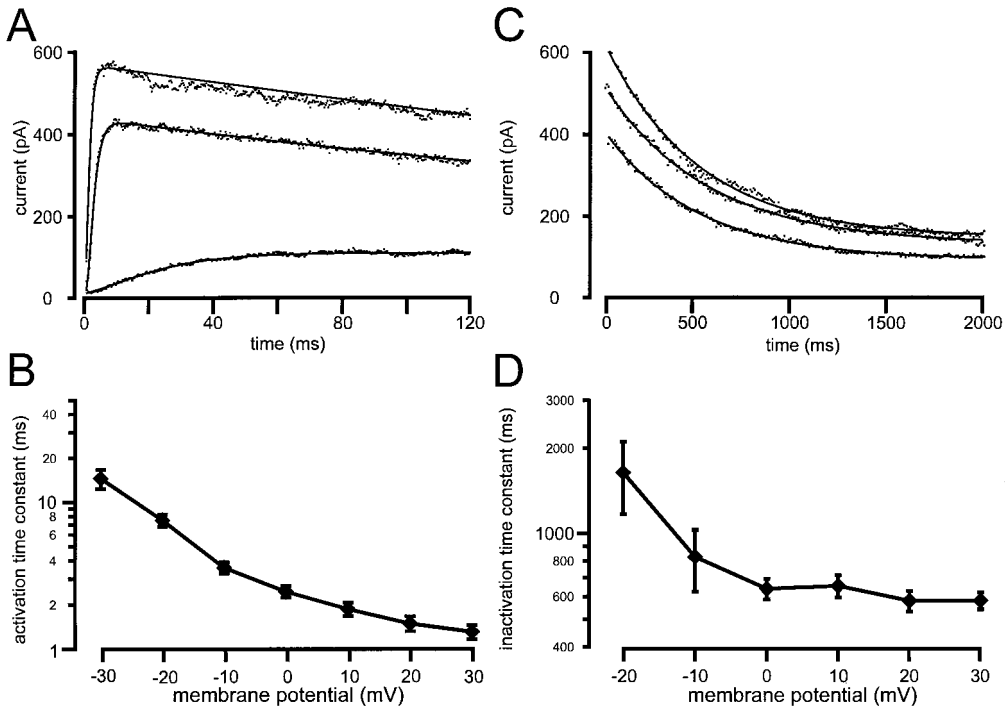

Fig. 6. Time-dependent activation and inactivation of DR currents. The time course of activation and inactivation of DR currents was fitted by Hodgkin-Huxley-kinetics (n^4j model). *A*: currents were evoked by 200-ms pulses to −30, 0, and +30 mV. Continuous lines represent the fitted curves. *B*: mean ± SE activation time constants from 22 cells are plotted as a function of membrane potential. *C*: cells were depolarized for 2,000 ms to potentials of −10, +10, and +30 mV. For each curve, the best fit of a single exponential to the inactivation time course is superimposed. *D*: mean ± SE inactivation time constants from 13 cells are plotted as a function of membrane potential.

Pharmacology of DR K^+ Currents

We investigated the sensitivity of DR channels in TGF-β-treated microglia to several peptide toxins. After extracellular application of 1 nM CTX, DR currents were inhibited by 60 ± 9% (n = 8), whereas CTX at 100 nM caused a nearly complete blockade of DR currents (Fig. 8, *A* and *D*).

Similar to the effect of CTX, extracellular KTX, applied at nanomolar concentrations, blocked DR currents of TGF-β-treated microglial cells (Fig. 8, *B* and *D*). When microglial cells were superfused with solutions containing 1 nM KTX, the mean amplitude of DR currents evoked by voltage steps to +30 mV was reduced by 54 ± 10% (n = 8). At 100 nM extracellular KTX, DR currents were almost completely blocked (by 93 ± 2%; n = 6) (Fig. 8*D*).

The snake toxin α-DTX was tested at concentrations of 10 and 100 nM. In contrast to the effects of CTX and KTX, both concentrations α-DTX inhibited DR currents only slightly, as shown in Fig. 8, *C* and *D*. At a test potential of +30 mV, DR currents were reduced on average by 17 ± 8% (n = 7) at 10 nM α-DTX and by 28 ± 7% (n = 13) at 100 nM α-DTX.

Identification and Regulation of K^+ Channel mRNA in TGF-β-Treated BV-2 Cells

The macroscopic and single channel behavior, including conductance, voltage dependence, time dependence, and pharmacological sensitivity, suggested that the IR channels were Kir2.1 and the DR channels were Kv1.3 in TGF-β1-treated microglial cells. We therefore conducted experiments to confirm this tentative identification of these channels and to explore whether changes in mRNA levels could account for the upregulation of DR currents.

The presence of Kv1.3 and Kir2.1 mRNA transcripts was tested with RT-PCR. DNA products apparently corresponding to these species were obtained after RT-PCR of total RNA when unique sets of primers were used. An image of a gel of the PCR products from one RNA sample after electrophoresis is shown in Fig. 9*A*. Also shown is the DNA band corresponding to G3PDH after RT-PCR. The sizes of the bands can be obtained by comparison with the molecular weight markers. When amplified with the primer set used, Kv1.3 is expected to give a band 479-bp long. Kir2.1 should be 376 bp, and G3PDH, 240 bp. The bands suggest that mRNA for these species are present. However, because a band could theoretically also be obtained through amplification of contaminating genomic DNA rather than mRNA, control reactions were performed in which the RT step was omitted. In these cases, the reaction remained at 4°C during the RT step. In the gel shown in Fig. 9*A*, the PCR product in the absence of RT was run in the lane to the right of that in which RT was performed. No DNA was amplified in the absence of

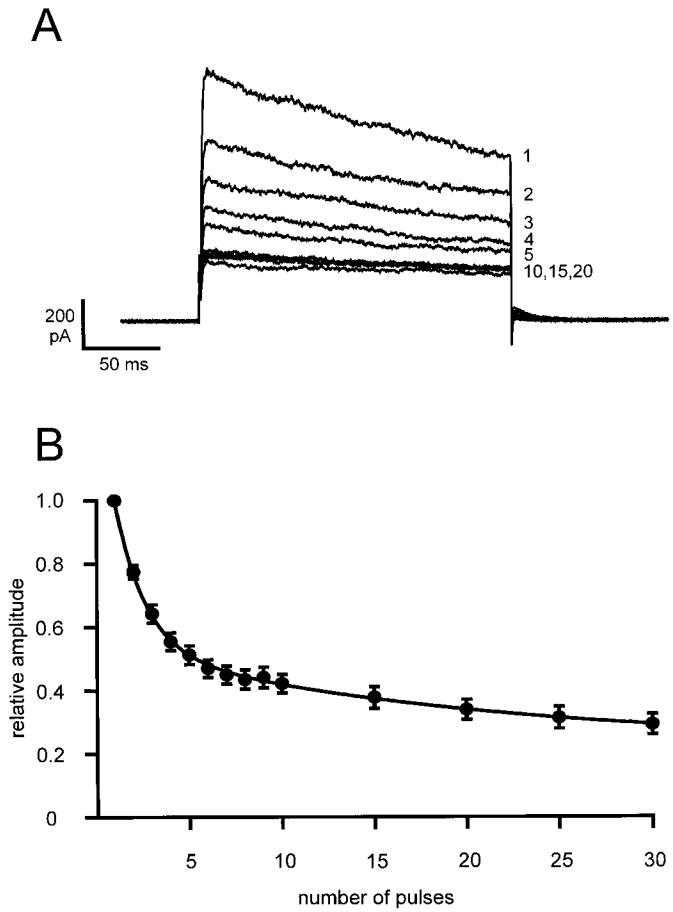

Fig. 7. Use dependence of DR K^+ currents. Microglial cells were stimulated by repetitive pulses from the holding potential (−60 mV) to +30 mV (200 ms) applied at a frequency of 1 Hz. *A*: example of current recordings. The numbers of the pulses are indicated. *B*: mean ± SE normalized peak current amplitudes in 17 cells are plotted as a function of the number of applied pulses.

RT, indicating that the amplified DNA originated from mRNA.

Restriction analysis was performed to determine whether the DNA obtained by RT-PCR had the base sequence expected for the Kv1.3 transcript. The DNA product was reamplified and subjected to digestion with either *Rsa* I, *Sac* I, or *Hph* I. A gel of the full-length DNA and products after digestion and electrophoresis is shown in Fig. 9*B*. *Rsa* I would be expected to cut the DNA into fragments of 376 and 103 bp. Exposure to *Sac* I would result in fragments of 425 and 54 bp. The fragments after digestion with *Hph* I should be 244 and 235 bp. In each case, the expected fragments were found. The most likely origin of the cDNA is, therefore, mouse Kv1.3.

The change in current density of the DR current in response to the addition of TGF-β1 to the growth media could be mediated by a change in the abundance of Kv1.3 transcript. To test this idea, the abundance of the transcript in the TGF-β-treated and untreated cells was compared using a competitive RT-PCR assay. A typical experiment is shown in Fig. 10. A sample of total RNA was isolated from each of the two cultures. RT-PCR was performed in a set of four reaction tubes for each sample. Total RNA was fixed in each reaction tube. However, a variable amount of competitor RNA was added to different tubes in each set before RT. The image of the gel after RT-PCR of Kv1.3, electrophoresis, and staining is shown in Fig. 10*A*. The amount of final product of the target or competitor is proportional to the intensity of the band. The ratio of the target to the competitor increased as the competitor in the reaction was reduced. For any competitor concentration, the ratio of target to competitor was higher in the reaction from the RNA sample obtained from the cells treated with TGF-β1. These ratios are plotted in Fig. 10*B* as a function of the concentration of Kv1.3 competitor added. The point of equal amplification of the two products occurs when the ratio of the target to competitor equals one (ignoring the difference in size). The amount of competitor added for this value is the amount of target in the sample. From the graph it is

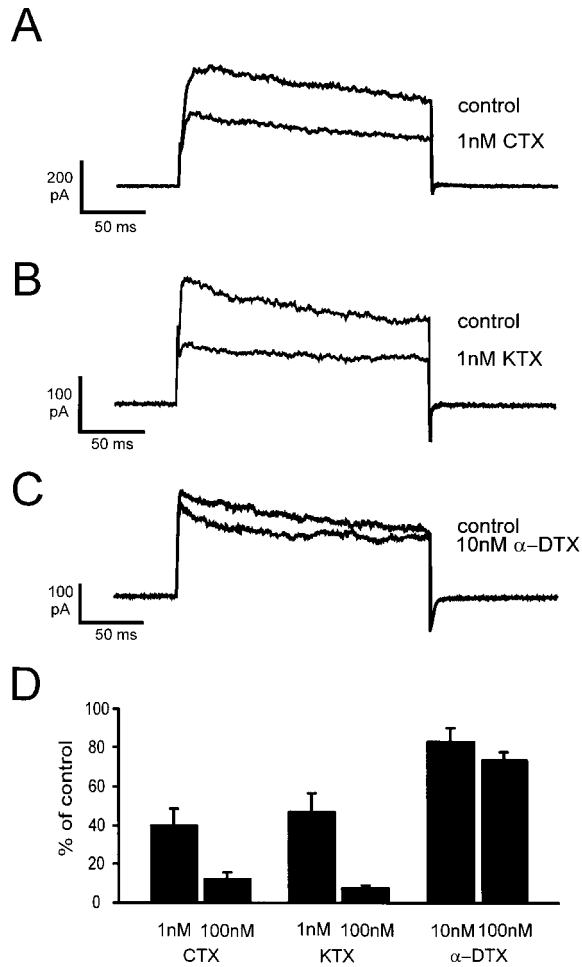

Fig. 8. Effects of peptide toxins on DR currents in TGF-β-treated microglia. DR currents evoked by voltage steps from the holding potential (−60 mV) to +30 mV for 200 ms are shown before and during superfusion with extracellular solution containing 1 nM charybdotoxin (CTX; *A*), 1 nM kaliotoxin (KTX; *B*), or 10 nM α-DTX (*C*). *D*: relative amplitude of peak DR currents (after leak subtraction) during superfusion with the indicated concentrations of CTX, KTX, or α-DTX.

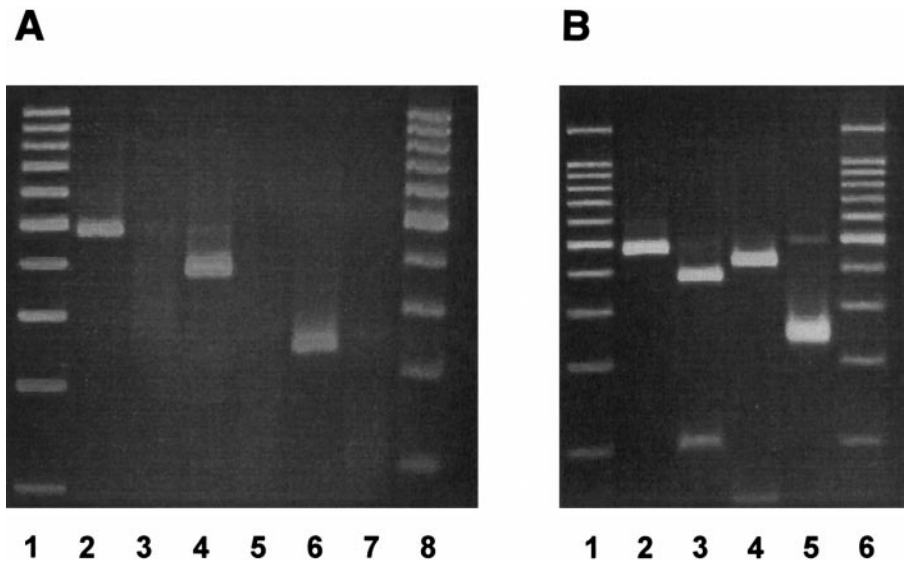

Fig. 9. RT-PCR test of the presence of potassium channel transcripts in BV-2 cells. *A*: an electrophoresis gel of the products of RT-PCR, applied to a sample of total RNA from BV-2 cells, is shown. Reactions were grouped into 3 sets of 2. Each set had a different primer pair. One PCR reaction in each set was done after a RT reaction (*lanes 2*, *4*, and *6*) and 1 was done in the absence of RT (*lanes 3*, *5*, and *7*). Primer sets used were expected to amplify Kv1.3 (*lanes 2* and *3*), Kir2.1 (*lanes 4* and *5*), or glyceraldehyde-3-phosphate-dehydrogenase (G3PDH; *lanes 6* and *7*). Note that the presence of cDNA for any product is dependent on the RT reaction. *B*: restriction analysis of the Kv1.3 cDNA. The full-length product was run in *lane 2* of the gel. Other lanes show fragments generated by treatment of the full-length cDNA with *Rsa* I (*lane 3*), *Sac* I (*lane 4*), or *Hph* I (*lane 5*). *Lanes 1* and *8* (*A*) or *6* (*B*) are 100-bp DNA markers. The 500-bp marker is more intense. The sizes of the cut fragments after exposure to restriction enzymes confirm the identity of the Kv1.3 cDNA product.

apparent that more competitor was added for equal amplification to the RT-PCR of the sample of TGF-β-treated cells. In the example assay shown, Kv1.3 transcript was a factor of 4.60 higher in the TGF-β-treated cells than in untreated microglial cells. To rule out the possibility that there are differences in RNA integrity between samples, one test is to determine whether there is a change in level of a species of mRNA not expected to be altered by the TGF-β1. A similar analysis of G3PDH abundance in the same samples (Fig. 10*C*) showed a small (23%) decrease in the cells exposed to TGF-β1. In three separate determinations, Kv1.3 mRNA abundance increased by an average factor of 4.67 ± 0.55. However, the abundance of the G3PDH transcript did not change (1.03 ± 0.18).

The competitive PCR method provides a good quantitative estimate of relative amounts of mRNA in different cell populations. By making several assumptions, it is possible to estimate the absolute numbers of Kv1.3 mRNA molecules in each cell. First, the efficiency of mRNA isolation is assumed to be 100%. Second, in contrast to difference measurements, the efficiency of RT-PCR of the target is assumed to be identical to that of the competitor. The control cells in the experiment in Fig. 10*B* had 11 mRNA molecules/cell, and the TGF-β1-treated cells had 56 mRNA molecules/cell. If the actual efficiency of isolation is <100% or if the efficiency of RT-PCR is less than the competitor, the true numbers of Kv1.3 mRNA molecules/cell would be proportionately higher.

Because immunofluorescence of Kv1.5 antibodies has been reported in rat microglia (21, 33), we used RT-PCR to probe for Kv1.5 mRNA in TGF-β-treated BV-2 cells. In three determinations, we could not detect mRNA for Kv1.5, although we did amplify G3DPH (as a control), and the primer set we used did amplify Kv1.5 from an identical amount of total RNA from mouse brain (data not shown).

DISCUSSION

In the present study we provide the first evidence that a deactivating cytokine is capable of changing the pattern of K^+ channel expression in microglia. We demonstrate that TGF-β induces upregulation of Kv1.3 mRNA and expression of the corresponding DR K^+ channels in murine microglia. The expression of IR channels was not affected by TGF-β.

Exposure of microglia to any of several different activating stimuli results in a characteristic pattern of parallel downregulation of IR channels and upregulation of DR channels. Thus large DR currents but no IR K^+ currents were detected in the majority of activated microglial cells grown with GM-CSF or stimulated with IFN-γ (13). A significantly reduced IR current density in parallel with an increased DR current density was observed in LPS-activated microglia (9, 31). The pattern of K^+ channel expression after treatment of microglia with the deactivating cytokine TGF-β differs in that DR upregulation occurred in the absence of any change in the expression of IR channels. Therefore, upregulation of DR channels in microglia is not obligatorily linked to downregulation of IR channels.

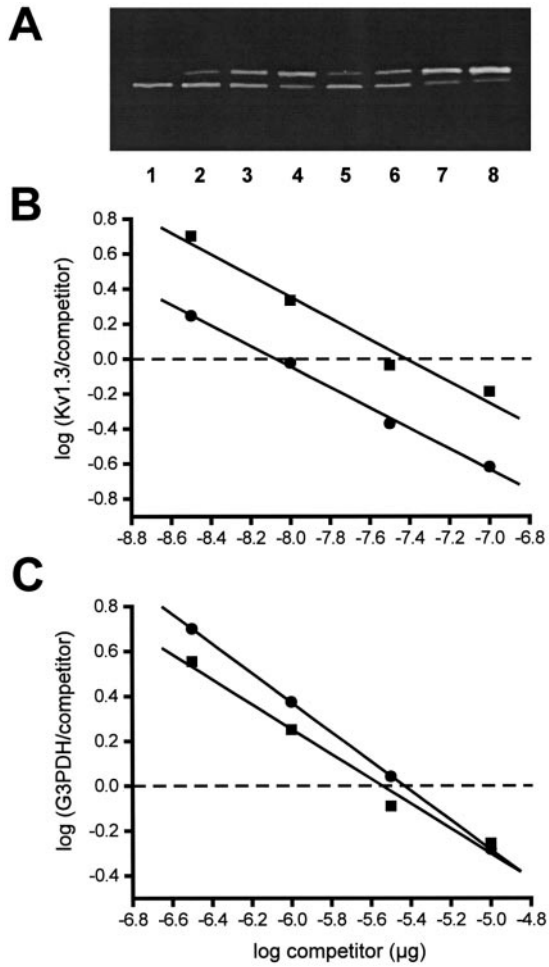

Fig. 10. Competitive RT-PCR reveals a selective increase in Kv1.3 mRNA abundance after treatment with TGF-β1. An example of a competitive RT-PCR assay to measure the difference in Kv1.3 and G3PDH mRNA between 2 total RNA samples is shown. *A*: an electrophoresis gel shows the products from 8 reactions. The *top* band in each lane is due to the presence of Kv1.3 target mRNA in any reaction, whereas the *bottom* band is due to Kv1.3 competitor RNA. The RNA sample from a control culture of BV-2 cells was used for the reactions giving products run in *lanes 1–4*. RNA from cells treated with TGF-β1 was used in the reactions with products in *lanes 5–8*. Competitor RNA was diluted, and the amount added to any reaction was 10^{-7} μg (*lanes 1* and *4*), 3.3×10^{-8} μg (*lanes 2* and *5*), 10^{-8} μg (*lanes 3* and *6*), or 3.3×10^{-9} μg (lanes 4 and *8*). The contrast of the image was increased for purposes of illustration. *B*: the ratio of Kv1.3 target to competitor from the reactions shown in *A* are plotted. The graph indicates that Kv1.3 mRNA was greater in the RNA sample from the TGF-β-treated cells. *C*: an RT-PCR assay to measure G3PDH mRNA in the 2 RNA samples used in analysis given in *A* and *B* is shown. There is little difference in G3PDH between the 2 RNA samples. ●, Untreated cells; ■, TGF-β1-treated cells

IR channels in TGF-β-treated microglia, similar to those of untreated microglia (10), were highly sensitive to extracellular Ba^{2+} but unaffected by δ-DTX, an inhibitor of ROMK-1 channels (19). The pharmacological properties together with the single channel conductance of ~30 pS suggests that Kir2.1 channels are expressed in TGF-β-treated microglial cells. With RT-PCR, we demonstrate the existence of Kir2.1 mRNA in control and TGF-β-treated microglia. Küst et al. (25) detected mRNA for ROMK-1 channels in rat microglia. On the basis of the pharmacological profile of the IR currents, it can be excluded that ROMK-1 channels are expressed to any significant extent in murine microglial cells before or after TGF-β treatment.

With respect to the single channel conductance, kinetic and pharmacological properties, DR K^+ currents in TGF-β-treated microglia closely resemble those in activated microglia (10) and in other macrophages (7, 15). We conclude that the same type of DR channel is upregulated in microglia after exposure to either deactivating or activating substances. We used RT-PCR to show that Kv1.3 mRNA is present in murine microglial cells and propose that it codes for the DR channels in TGF-β-treated microglia. This hypothesis is supported by our observation that the levels of mRNA for Kv1.3 increased on average 4.7-fold in microglia after treatment with TGF-β, i.e., changes in mRNA levels were similar to those in DR current density. It has been reported that antibodies to Kv1.5 as well as to Kv1.3 stained LPS-treated rat microglia (33) and rat microglia in cultured tissue prints (21). We found no electrophysiological evidence of significant expression of Kv1.5 channels in TGF-β-treated murine microglia. Both CTX and KTX, which inhibit Kv1.3 but not Kv1.5 (16), blocked nearly all of the outward current. Furthermore, we could not detect mRNA for Kv1.5 using RT-PCR in BV-2 microglial cells treated with TGF-β. In contrast with rat microglia, murine microglia evidently express Kv1.3 but not Kv1.5 K^+ channels.

Increases in Kv1.3 mRNA levels were seen in rat microglia after stimulation of adenosine A_{2a} receptors. Kv1.3 channel expression was detected by immunocytochemical methods, but no patch-clamp studies were performed, so a quantitative comparison of channel expression and mRNA levels is not possible (25). When THP-1 cells were induced to differentiate from monocytes into macrophages, downregulation of DR channels and upregulation of IR channels were paralleled by changes of the corresponding Kv1.3 and Kir2.1 mRNA levels (8). In rat microglia after stimulation with LPS, changes in Kv1.3 mRNA levels were not observed, although the proportion of cells expressing DR channels increased dramatically (30). When we used competitive PCR to examine mRNA levels more quantitatively, we found that mRNA levels for Kv1.3 in microglia changed in parallel with K^+ channel expression.

Because DR channels are upregulated in microglia stimulated with LPS, IFN-γ, or GM-CSF, it was proposed that the expression of DR channels is a marker for activated microglia (13, 31). Because the same Kv1.3 DR channel is also upregulated on deactivation by TGF-β, expression of this channel is not an unambiguous marker of activation of microglial cells. However, it is clear that the pattern of K^+ channel expression changes predictably with a variety of stimuli. Perhaps DR channel expression is upregulated during changes from one functional state to another rather than in a defined functional state of microglial cells. This idea is supported by the finding that ramified resting microglia upregulated DR channels immedi-

ately after exposure to astrocyte-conditioned medium but no longer expressed DR currents several days after treatment with astrocyte-conditioned medium (12).

A specific role for K^+ channels in microglial signaling remains to be established. Pharmacological lesion experiments suggest that Kv1.3 channels may play a permissive role in proliferation of microglia (21), similar to that in T lymphocytes (6). One general function of K^+ channels in leukocytes is to maintain a large driving force for Ca^{2+} influx through calcium-release-activated Ca^{2+} channels (26). When K^+ channels open, they drive the membrane potential toward the Nernst potential for K^+, which is usually negative to the resting membrane potential. Further experiments are required to demonstrate a similar functional role of Kv1.3 channels in microglia. Leukocytes expressing IR K^+ channels have more negative resting membrane potentials than cells with only Kv1.3 K^+ channels, suggesting that cells express IR K^+ channels when they need a very negative resting potential and DR K^+ channels if they need a moderately negative resting potential (7). The finding that resting membrane potential and expression levels of IR channels remained unchanged in microglia after exposure to TGF-β (data not shown) or to astrocyte-conditioned medium (12) indicates that IR channels determine the resting membrane potential of untreated and deactivated microglial cells. That DR K^+ channels activate with depolarization means that they have a much greater capacity than IR K^+ channels to resist depolarizing influences. The change in expression of K^+ channels in response to TGF-β is different from that with activating stimuli, because IR channels are not downregulated. These cells may, therefore, have a rather negative membrane potential and be resistant to depolarization. It should be noted that both deactivating cytokines such as TGF-β and activating stimuli such as LPS have several effects in common, including reduction of proliferation. In addition, activating stimuli may lead to release of TGF-β from microglial cells (22).

The authors thank Sieglinde Latta for the preparation of cell cultures and Astrid Düerkop for technical assistance.

This work was supported in part by the Deutsche Forschungsgemeinschaft Grant SFB 507/C3 (to C. Eder and U. Heinemann), the Michael Reese Health Trust (to F. N. Quandt), Research Grant HL-52671 from the National Heart, Lung, and Blood Institute (NHLBI) (to T. E. DeCoursey), and NHLBI Training Grant HL-07692 (to W. Zhou).

REFERENCES

1. **Blasi E, Barluzzi R, Bocchini V, Mazzolla R, and Bistoni F.** Immortalization of murine microglial cells by a v-*raf*/v-*myc* carrying retrovirus. *J Neuroimmunol* 27: 229–237, 1990.
2. **Bocchini V, Mazzolla R, Barluzzi R, Blasi E, Sick P, and Kettenmann H.** An immortalized cell line expresses properties of activated microglial cells. *J Neurosci Res* 31: 616–621, 1992.
3. **Cahalan MD, Chandy KG, DeCoursey TE, and Gupta S.** A voltage-gated potassium channel in human T lymphocytes. *J Physiol (Lond)* 358: 197–237, 1985.
4. **Chomczynski P.** A reagent for the single-step simultaneous isolation of RNA, DNA and proteins from cell and tissue samples. *Biotechniques* 15: 532–537, 1993.
5. **Constam DB, Philipp J, Malipiero UV, ten Dijke P, Schachner M, and Fontana A.** Differential expression of transforming growth factor-β1, -β2, and -β3 by glioblastoma cells, astrocytes, and microglia. *J Immunol* 148: 1404–1410, 1992.
6. **DeCoursey TE, Chandy KG, Gupta S, and Cahalan MD.** Voltage-gated K^+ channels in human T lymphocytes: a role in mitogenesis? *Nature* 307: 465–468, 1984.
7. **DeCoursey TE and Grinstein S.** Ion channels and carriers in leukocytes. In: *Inflammation: Basic Principles and Clinical Correlates* (3rd ed.), edited by Gallin JI and Snyderman R. Philadelphia, PA: Lippincott Williams & Wilkins, 1999, p. 639–659.
8. **DeCoursey TE, Kim SY, Silver MR, and Quandt FN.** Ion channel expression in PMA-differentiated human THP-1 macrophages. *J Membr Biol* 152: 141–157, 1996.
9. **Draheim HJ, Prinz M, Weber JR, Weiser T, Kettenmann H, and Hanisch UK.** Induction of potassium channels in mouse brain microglia: cells acquire responsiveness to pneumococcal cell wall components during late development. *Neuroscience* 89: 1379–1390, 1999.
10. **Eder C.** Ion channels in microglia (brain macrophages). *Am J Physiol Cell Physiol* 275: C327–C342, 1998.
11. **Eder C, Fischer HG, Hadding U, and Heinemann U.** Properties of voltage-gated potassium currents of microglia differentiated with granulocyte/macrophage colony-stimulating factor. *J Membr Biol* 147: 137–146, 1995.
12. **Eder C, Schilling T, Heinemann U, Haas D, Hailer N, and Nitsch R.** Morphological, immunophenotypical and electrophysiological properties of resting microglia in vitro. *Eur J Neurosci* 11: 4251–4261, 1999.
13. **Fischer HG, Eder C, Hadding U, and Heinemann U.** Cytokine-dependent K^+ channel profile of microglia at immunologically defined functional states. *Neuroscience* 64: 183–191, 1995.
14. **Flanders KC, Ren RF, and Lippa CF.** Transforming growth factor-βs in neurodegenerative disease. *Prog Neurobiol* 54: 71–85, 1998.
15. **Gallin EK.** Ion channels in leukocytes. *Physiol Rev* 71: 775–811, 1991.
16. **Grissmer S, Nguyen AN, Aiyar J, Hanson DC, Mather RJ, Gutman GA, Karmilowicz MJ, Auperin DD, and Chandy KG.** Pharmacological characterization of five cloned voltage-gated K^+ channels, types Kv1.1, 1.2, 1.3, 1.5, and 3.1, stably expressed in mammalian cell lines. *Mol Pharmacol* 45: 1227–1234, 1994.
17. **Hamill OP, Marty A, Neher E, Sakmann B, and Sigworth FJ.** Improved patch-clamp techniques for high-resolution current recording from cells and cell-free membrane patches. *Pflügers Arch* 391: 85–100, 1981.
18. **Hodgkin AL and Huxley AF.** A quantitative description of membrane current and its application to conduction and excitation in nerve. *J Physiol (Lond)* 117: 500–544, 1952.
19. **Imredy JP, Chen C, and MacKinnon R.** A snake toxin inhibitor of inward rectifier potassium channel ROMK1. *Biochemistry* 37: 14867–14874, 1998.
20. **Jones LL, Kreutzberg GW, and Raivich G.** Transforming growth factor β's 1, 2 and 3 inhibit proliferation of ramified microglia on an astrocyte monolayer. *Brain Res* 795: 301–306, 1998.
21. **Kotecha SA and Schlichter LC.** A Kv1.5 to Kv1.3 switch in endogenous hippocampal microglia and a role in proliferation. *J Neurosci* 19: 10680–10693, 1999.
22. **Kreutzberg GW.** Microglia: a sensor for pathological events in the CNS. *Trends Neurosci* 19: 312–318, 1996.
23. **Krieglstein K, Rufer M, Suter-Crazzolara C, and Unsicker K.** Neural functions of the transforming growth factors β. *Int J Dev Neurosci* 13: 301–315, 1995.
24. **Kubo Y, Baldwin TJ, Jan YN, and Jan LY.** Primary structure and functional expression of a mouse inward rectifier potassium channel. *Nature* 362: 127–133, 1993.
25. **Küst BM, Biber K, van Calker D, and Gebicke-Haerter PJ.** Regulation of K^+ channel mRNA expression by stimulation of

adenosine A_{2a}-receptors in cultured rat microglia. *Glia* 25: 120–130, 1999.
26. **Lewis RS and Cahalan MD.** Mitogen-induced oscillations of cytosolic Ca^{2+} and transmembrane Ca^{2+} current in human leukemic T cells. *Cell Regul* 1: 99–112, 1989.
27. **Loughlin AJ, Woodroofe MN, and Cuzner ML.** Modulation of interferon-γ-induced major histocompatibility complex class II and Fc receptor expression on isolated microglia by transforming growth factor-β1, interleukin-4, noradrenaline and glucocorticoids. *Immunology* 79: 125–130, 1993.
28. **McRae A, Dahlström A, and Ling EA.** Microglia in neurodegenerative disorders: emphasis on Alzheimer's disease. *Gerontology* 43: 95–108, 1997.
29. **Merrill JE and Zimmerman RP.** Natural and induced cytotoxicity of oligodendrocytes by microglia is inhibitable by TGF-β. *Glia* 4: 327–331, 1991.
30. **Nörenberg W, Appel K, Bauer J, Gebicke-Haerter PJ, and Illes P.** Expression of an outwardly rectifying K^+ channel in rat microglia cultivated on teflon. *Neurosci Lett* 160: 69–72, 1993.
31. **Nörenberg W, Gebicke-Haerter PJ, and Illes P.** Voltage-dependent potassium channels in activated rat microglia. *J Physiol (Lond)* 475: 15–32, 1994.
32. **Price RW, Brew B, Sidtis J, Rosenblum M, Scheck AC, and Cleary P.** The brain in AIDS: central nervous system HIV-1 infection and AIDS dementia complex. *Science* 239: 586–592, 1988.
33. **Pyo H, Chung S, Jou I, Gwag B, and Joe EH.** Expression and function of outward K^+ channels induced by lipopolysaccharide in microglia. *Mol Cell* 7: 610–614, 1997.
34. **Raivich G, Bohatschek M, Kloss CUA, Werner A, Jones LL, and Kreutzberg GW.** Neuroglial activation repertoire in the injured brain: graded response, molecular mechanisms and cues to physiological function. *Brain Res Rev* 30: 77–105, 1999.
35. **Schilling T, Cherny VV, Zhou W, Quandt FN, Heinemann U, DeCoursey TE, and Eder C.** TGF-β upregulates Kv1.3 channels in microglia (Abstract). *Biophys J* 78: 207A, 2000.
36. **Schilling T, Cherny VV, Zhou W, Quandt FN, Heinemann U, DeCoursey TE, and Eder C.** K^+ channel expression in deactivated microglia (Abstract). *Pflügers Arch* 439: R428, 2000.
37. **Siebert PD and Larrick JW.** Competitive PCR. *Nature* 359: 557–558, 1992.
38. **Silver MR, Shapiro MS, and DeCoursey TE.** Effects of external Rb^+ on inward rectifier K^+ channels of bovine pulmonary artery endothelial cells. *J Gen Physiol* 103: 519–548, 1994.
39. **Stoll G and Jander S.** The role of microglia and macrophages in the pathophysiology of the CNS. *Prog Neurobiol* 58: 233–247, 1999.
40. **Streit WJ, Walter SA, and Pennell NA.** Reactive microgliosis. *Prog Neurobiol* 57: 563–581, 1999.
41. **Suzumura A, Sawada M, Yamamoto H, and Marunouchi T.** Transforming growth factor-β suppresses activation and proliferation of microglia in vitro. *J Immunol* 151: 2150–2158, 1993.
42. **Woodroofe MN, Bellamy AS, Feldman M, Davison AN, and Cuzner ML.** Immunocytochemical characterisation of the immune reaction in the central nervous system in multiple sclerosis: possible role for microglia in lesion growth. *J Neuro Sci* 74: 135–152, 1986.
43. **Zhou H, Chepilko S, Schutt W, Choe H, Palmer LG, and Sackin H.** Mutations in the pore region of ROMK enhance Ba^{2+} block. *Am J Physiol Cell Physiol* 271: C1949–C1956, 1996.